arXiv:1003.3789v1 [cond-mat.soft] 19 Mar 2010

Transport coefficients of soft sphere fluids at high densities

Yu. D. Fomin, V. V. Brazhkin, and V. N. Ryzhov
Institute for High Pressure Physics, Russian Academy of Sciences, Troitsk 142190, Moscow Region, Russia
(Dated: March 22, 2010)

Molecular dynamics computer simulation has been used to compute the self-diffusion coefficient, and shear viscosity of soft-sphere fluids, in which the particles interact through the soft-sphere or inverse power pair potential. The calculations have been made along the melting line in a wide range of pressures and temperatures. The validity of scaling relations for thermodynamic parameters and kinetic coefficients was checked. It was shown that the Stokes-Einstein relationship is obeyed if the Barker diameter is used as a characteristic length scale. It was also shown that the viscosity is non-monotonic along the isochores as predicted by Ya. Rosenfeld. It was shown that the viscosity is strongly growing along the melting line, however, this increase does not stimulate the glass transition because the relaxation time is decreasing.

PACS numbers: 61.20.Gy, 61.20.Ne, 64.60.Kw

I. INTRODUCTION

Knowledge of transport coefficients is extremely important for characterizing the properties of liquid. They allow one to characterize how fast the dynamics of the liquid is. Because of this, transport coefficients are intensively studied experimentally, theoretically and by simulations. The most important transport property for an experimental study is viscosity. Viscosity can easily be measured by a number of techniques. Nevertheless many questions on the behavior of viscosity as a function of pressure and temperature still remain. Some of them are considered in the present article.

It is well known that the viscosity of most liquids grows exponentially with increasing pressure at constant temperature and demonstrates critical behavior in the vicinity of the glass transition line. In the case of hard or soft spheres the glass transition at high pressures corresponds to the jamming of the system. However, such kind of behavior is typical for supercooled liquids while the behavior of viscosity close to the melting line is not clear.

As was discussed in [1], there are two empirical approaches to the description of the viscosity behavior of simple liquids under simultaneous changes of temperature and pressure. The first approach goes back to Bridgman's works [2] and suggests that the viscosity of the liquid is nearly constant along the isochores. The other and currently more widespread approach was formulated by Pourier [3]. It is based on the presumption that the viscosity of the melts is invariable along the melting curve. The experimental data analysis shows that both approaches are incorrect; the constant viscosity lines for rare gas liquids, as well as for liquid metals, have a slope that is intermediate between the melting line and the isochore slopes [4] (figure 5). As a consequence, the viscosity of simple melts along the melting curve increases and this increase can be extrapolated to megabar pressures [4]. However, this extrapolation is in fact difficult because of a rather small viscosity variation in the covered range [5]. For example, the viscosity of the Fe melt grows along the melting curve by several times with the pressure increase to $10-15$ GPa [5, 6]. However, the obtained data do not permit drawing any conclusions with regard to the character of this growth; various analytic models equally closely descriptive of the studied baric dependencies give different extrapolation results. In consequence, different equations employed in the extrapolation of the Fe melt viscosity to pressures of $1.4-3.1$ Mbar, corresponding to the conditions existing in the Earth's outer core, provide the data that vary over $10-20$ orders of magnitude [5] (figure 6). The same is valid for other simple melts like liquid Ar.

Thus, it is presently impossible to draw inferences about how high the viscosity can grow along the melting curve for the given melts with the pressure increase to about $100-1000$ GPa. If the viscosity growth is minor, liquid metals and rare gas liquids will remain very poor glass formers at megabar pressures. On the other hand, the viscosity growth along the melting curve amounts to several orders of magnitude, so the question arises whether the liquid metals and rare gas liquids become viscous glass-forming systems under the increasing pressure. In this case, the glass transition of the given melts in the megabar range should be similar to the jamming of soft spheres.

The main purpose of this paper is the computer simulation study of the behavior of the transport coefficients of a soft sphere system in a wide range of densities and temperatures. Although the interatomic potential in liquid metals can not be described by a pair potential, the potential in rare gas liquids can be approximated by the Lennard-Jones function which can be substituted in the high density and temperature limit by a soft sphere potential. In this respect it is interesting to carry out a systematic study of the transport coefficients of soft sphere system as a generic model for real liquids at high pressure.

Note that most of previous studies of transport coefficients of liquids were concerned to the low density - low temperature region while high density - high temperature properties were beyond the consideration. Only few works on the high density transport properties are available (see, for example, [7]) In this sense the present work is directed to fill this gap.

II. SOFT SPHERES: THEORETICAL APPROACH

Interestingly, one can make some important predictions about thermodynamic properties of soft spheres on the basis of the form of the potential only. To do this one can use the Klein theorem [9, 10].

Consider the dimensionless density $\rho\frac{\sigma^3}{V}$ and reduced coordinates $s = r(\frac{N}{V})^{1/3}$. The partition function of soft spheres in these variables has the following form [11]:

$$Z = \frac{V^N}{N\lambda^{3N}} \int_{s_1} ... \int_{s_N} exp[-\beta\rho^{n/3} \sum_{i<j} s_{ij}^{-n}] ds_1 ... ds_N, \tag{1}$$

where $\lambda = \left(\frac{\hbar}{2\pi m k_B T}\right)^{1/2}$ is de Broile wave length and $\beta = 1/(k_B T)$. The Klein theorem states that if U is a homogeneous function of degree n, i.e. $U(\lambda r_1, ..., \lambda r_N) = \lambda^n U(r_1, ..., r_N)$ then for N sufficiently large [10]

$$\int_{r_1} ... \int_{r_N} exp[-\beta \cdot U(r_1, ..., r_N)] dr_1 ... dr_N = G(\beta \cdot \rho^{-n/3}), \tag{2}$$

where G is some function of $(\beta\rho^{-n/3})$.

Using the Klein theorem one can find that the equation of state has the form:

$$\frac{PV}{Nk_BT} = 1 + \phi(\rho(\frac{\varepsilon}{k_BT})^{3/n}). \tag{3}$$

If the system with such equation of state has a first order phase transition (let us call it melting), then the transition line is characterized by the universal parameter $\rho(\frac{\varepsilon}{k_BT})^{3/n}$ [11]. From this it follows that the densities of a liquid and crystal along the melting line are:

$$\rho_l = c_l(\frac{k_BT}{\varepsilon})^{3/n} \tag{4}$$

$$\rho_c = c_c(\frac{k_BT}{\varepsilon})^{3/n}, \tag{5}$$

where c_l and c_c are constants. One can see that the densities along the melting line follow some scaling law.

This approach was further developed in the work [12], where the scaling relations were derived under the assumption of scaling invariancy of the Hamilton equations for homogeneous potentials.

Remember that kinetic energy is a homogeneous function of the power 2:

$$K(ap_i) = a^2 K(p_i) \tag{6}$$

If scaling $r_i = ar_i$, $p_i = bp_i$ and $t = ct$ with $b^2 = a^{-n}$ and $c^2 = a^{2+n}$ is applied then the new phase trajectory of the system has the same geometric shape [12]. Then the following scaling laws are valid (we skip the Boltzmann constant in the formulas below for the sake of brevity):

$$V = a^3 V_0 \tag{7}$$

$$T = \frac{2}{3N}\langle\sum \frac{p_i^2}{2m_i}\rangle \longrightarrow T = a^{-n}T_0 \longrightarrow V = V_0\left(\frac{T}{T_0}\right)^{-3/n} \tag{8}$$

$$P = \frac{NT}{V} - \frac{1}{3V}\langle\sum q_i \frac{\partial U}{\partial q_i}\rangle \longrightarrow P = P_0\left(\frac{T}{T_0}\right)^{1+3/n}. \tag{9}$$

Using the Green - Kubo relations for the diffusion $D = \int_0^\infty < \mathbf{V}(t)\mathbf{V}(0) > dt$ and viscosity $\eta = \frac{1}{Vk_BT}\int_0^\infty < \sigma^{xy}(t)\sigma^{xy}(0) >$, where σ^{xy} is a stress tensor component, one can derive the scaling relations for diffusion and viscosity:

$$\eta \sim P^{\frac{n+4}{2n+6}} \tag{10}$$

or

$$\eta \sim T^{\frac{n+4}{2n}}, \tag{11}$$

and

$$D \sim P^{\frac{n-2}{2(n+3)}} \tag{12}$$

or

$$D \sim T^{1/2-1/n}. \tag{13}$$

Below we compute different quantities in simulation and fit the results to the corresponding scaling law using the least square procedure.

One can see that, following [12], the scaling relations can be generalized to be applicable to the transport coefficients, however this approach involves some assumptions which are not fully proved. This is why it is particularly interesting to check whether the scaling predictions for the transport coefficients are correct.

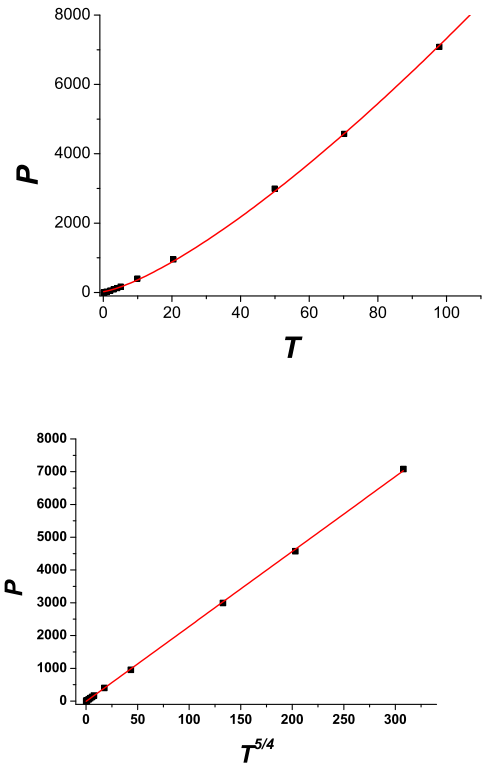

FIG. 1: Pressure as a function of temperature along the melting line in usual (a) and scaled (b) forms. The symbols are MD data and the line is the scaling law fitting.

III. SIMULATION

In the present work we study the viscosity, η_s, and diffusivity, D, of soft spheres. The choice of the system is determined by the following reasons. In order to investigate the behavior of the system along the melting line in a wide range of pressures we need to know the phase diagram of the system including a high pressure region. In most cases the melting lines were studied in the vicinity of the triple points. As it was shown that the soft sphere system obeys the scaling law. The parameters of the scaling of pressure and density with temperature along the melting line were determined both from simulation [13] and from density functional theory [14].

The soft sphere potential has the form:

$$\Phi(r) = \varepsilon \left(\frac{\sigma}{r}\right)^n. \qquad (14)$$

In our simulations we use $n = 12$. The potential is cut at the distance $r_c = 2.5$ as in standard simulations of Lennard-Jonse systems. Reduced units ($\varepsilon = 1$ and $\sigma = 1$) are used in the paper. As it was shown (see, for example, previous section and [13]), the behavior of soft spheres system depends on the parameter $\gamma_n = \rho\sigma^3(\frac{k_B T}{\varepsilon})^{-3/n}$. In [13] it was shown that the line of fluid to solid transition is $\gamma_n = 1.15$. From this formula one can compute the transition density to be used in simulations.

The system of 1000 particles was simulated in the microcanonical (constant N, V and E) ensemble. Equations of motion were integrated by the velocity Verlet algorithm. The equilibration time was set to $5 \cdot 10^5$ time steps and the production time - $3.5 \cdot 10^6$ steps. The time step we use is $dt = 0.0005$. During equilibration the velocity rescaling was applied to keep the temperature constant. During the production cycle, the NVE ensemble was used. The diffusion coefficient was calculated from the mean square displacement via Einstein relation, while the viscosity was determined by the integration of the stress correlation function [8].

The computation of the phase diagram of the system was also done. The reason for this computation is as follows. To our knowledge, all previous works studying soft sphere phase diagram considered the system at temperatures of the order of unity. Although it allows finding the scaling coefficient γ_n, the value may contain some errors. Since in the present work we study the temperatures up to $T = 100$, these small errors can give quite large uncertainty in the location of the melting line.

Because of this we computed the melting densities at $T = 20$ and $T = 50$. The same system of 1000 particles was used for this calculation in the case of the liquid and of 1372 particles for the FCC solid. The transition points were determined via the double tangent construction to the free energy lines. The crystal free energy was computed by coupling to the Einstein crystal [8], while the liquid free energy was determined by integrating the equation of state from the dilute gas limit [8]. Table 1 presents a comparison of the melting points obtained by our simulations to the predictions based on the scaling factor from Ref. [13].

T	ρ_l (this work)	ρ_l (ref. [13])	relative discrepancy
20	2.45	2.43	0.8%
50	3.12	3.06	1.6%

We can see that the agreement is rather good. It confirms that one can use the scaling parameters from the reference [13].

IV. RESULTS AND DISCUSSION

Transport Coefficients Behavior

The main purpose of this paper is to study the behavior of transport coefficients - shear viscosity and diffusion - in a wide range of densities and temperatures. To do this, we measure transport coefficients along the melting line and along a set of isochores for temperatures ranging from $T = 0.1$ up to $T = 100.0$. The following isochores are considered: $\rho = 0.65; 0.95; 1.51; 2.43; 2.69; 2.89; 3.06; 3.2; 3.33; 3.44$. Note that the density and temperature dependence of pressure

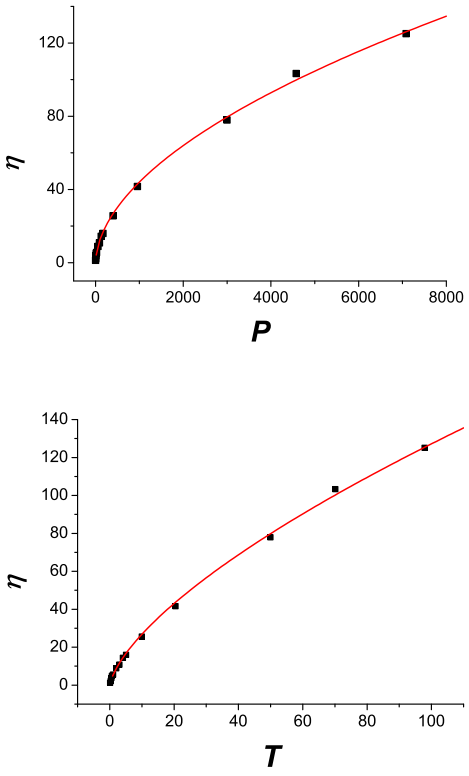

FIG. 2: Viscosity along the melting line as a function of pressure and temperature. The symbols are the MD data and the line is the scaling law fitting.

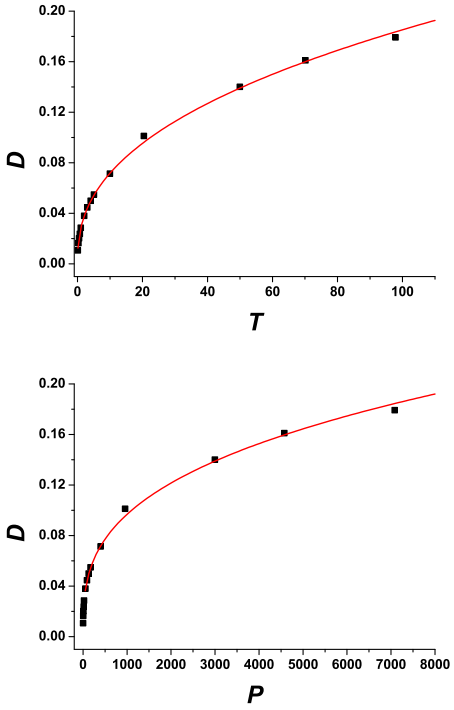

FIG. 3: Diffusion coefficient along the melting line as a function of pressure and temperature . The symbols are the MD data and the line is the scaling law fitting.

is rather strong; thus, the investigated density and temperature range corresponds to the pressure range varying from about unity to about 7000. Changing Lennard-Jones reduced units to real ones, we have the pressure varying in the range up to 300GPa. It covers almost the entire range of experimentally attainable static high pressures.

Figs. 1a and 1b present the pressure dependence along the melting line in usual and scaled forms. One can see that the scaling law works well.

The next figures (Figs. 2a and 2b) show the behavior of viscosity along the melting line as functions of both pressure and temperature and the fitting to the corresponding scaling formulas. As one can see, the scaling rules for viscosity are well fulfilled too. Unlike some predictions, the viscosity is not constant along the melting line. The mechanism of the viscosity growth will be discussed below.

Finally, Figs. 3a and 3b present the diffusion coefficient along the melting line.

Figs. 2 and 3 show the diffusion and viscosity growth along the melting line. Although it may seem counter intuitive, they satisfy to the scaling laws. We will discuss this problem below.

Figs.4a and 4b show the diffusion coefficient along different isochores and along the melting line as functions of temperature and pressure. As one can expect the diffusion increases upon temperature growth while at fixed temperature it decreases with increasing density. Diffusion also increases with increasing pressure along the isochores because in this situation we have simultaneous increase of temperature.

The behavior of viscosity along the isochores is more complex (Figs. 5a and 5b). One can see from the insets in the figures that the viscosity is not a monotonic function of pressure and temperature. The viscosity decreases with pressure close to the melting line, and increases away from it. Another conclusion from these figures is that the viscosity behaves qualitatively similar along different isochores - the shapes of the curves are almost the same for different densities.

A possible explanation of the nonmonotonic behavior of the viscosity was suggested by Rosenfeld [15]. In his works [15, 16] Rosenfeld showed the connection between transport coefficients of a fluid and excess entropy. Considering the behavior of the entropy he showed that the viscosity can have a minimum. He also gave a qualitative explanation of this fact. If we consider viscosity as an integral over stress correlation function, we can split it to three contributions: kinetic - kinetic (kk), kinetic - potential (kp) and potential - potential (pp)[8, 17]:

$$\eta = \int_0^\infty C_{kk}(t)dt + \int_0^\infty C_{kp}(t)dt + \int_0^\infty C_{pp}(t)dt, \quad (15)$$

where

$$C_{kk}(t) = \frac{m^2\rho}{Nk_BT}\sum_{i=1}^{N}\sum_{j=1}^{N} < v_{x,i}(0)v_{y,i}(0)v_{x,j}(y)v_{y,j}(y) >, \quad (16)$$

where $v_{x,i}(t)$ denotes x component of the velocity of the particle i at time t.

$$C_{pk}(t) = \frac{2m\rho}{Nk_BT}\sum_{i=1}^{N}\sum_{j=1}^{N}\sum_{k=1,k\neq j}^{N}\langle v_{x,i}(0)v_{y,i}(0)\cdot\frac{x_{jk}(t)y_{jk}(t)}{r_{jk}(t)^2}F[r_{jk}(t)]\rangle, \quad (17)$$

where $x_{jk}(t)$ and $y_{jk}(t)$ are Cartesian components of $\mathbf{r}_{jk}(t)$ and $F(r) = -\frac{r}{2}\frac{\partial\Phi[r]}{\partial r}$ - force between particles j and k.

Finally

$$C_{pp}(t) = \frac{\rho}{Nk_BT}\sum_{i=1}^{N}\sum_{j=1,j\neq i}^{N}\sum_{k=1}\sum_{l=1,l\neq k}^{N}\langle\frac{x_{ij}(0)y_{ij}(0)}{r_{ij}(0)^2}F[r_{ij}(0)]\cdot\frac{x_{kl}(t)y_{kl}(t)}{r_{kl}(t)^2}F[r_{kl}(t)].\rangle. \quad (18)$$

The role of different contributions to the viscosity for a Lennard - Jones fluid was studied by several authors (see, for example, [18, 19]).

One can expect that close to the melting line the main contribution to the viscosity comes from the potential - potential correlation, while at high temperatures the kinetic - kinetic part should be dominant. Having the pp correlation decreasing and the kk one increasing, we can expect that a minimum of the total viscosity can be observed.

In order to verify this suggestion we carried out the calculations of the different contributions to the viscosity for the density $\rho = 1.51$ and a set of temperatures (pressures) (Figs. 6a and 6b). As one can see from these figures the suggestion is correct: while the pp contribution decreases with increasing temperature both the kk and kp ones increase. Because of this one can expect the further increase of the viscosity with increasing temperature.

Given this increase of the viscosity, one can pose a question about a glass transition in the soft sphere system. Two definitions of the glass transition point are common: the one which is connected to the relaxation time of the system, and another which defines the glassification through the viscosity increase. The Maxwell relaxation time and shear viscosity are related via the equation [17]:

$$\tau = \eta/G_{inf} \quad (19)$$

where

$$G_{inf} = \rho k_BT + \frac{2\pi\rho^2}{15}\int_0^\infty drg(r)\frac{d}{dr}(r^4\frac{d\Phi}{dr}) \quad (20)$$

is the infinite-frequency shear modulus [20, 21].

The behavior of the elastic modulus G_{inf} along the melting line is shown in Fig.7. One can see that G_{inf} grows dramatically. Fig. 8 presents the relaxation time along the melting line. As it is clear from this plot, although the viscosity of the system increases with increasing temperature along the melting line the relaxation time becomes very small. Having small relaxation time, the system can definitely not become glasslike.

One can conclude that the main glassification criterion is the one through the relaxation time. As a result, even at certain conditions one has the viscosity increase, at the same time the high viscosity does not mean glassification because of decrease of the relaxation time. It seems that it is a high pp viscosity that brings the system to glass transition while dominating kk viscosity does not.

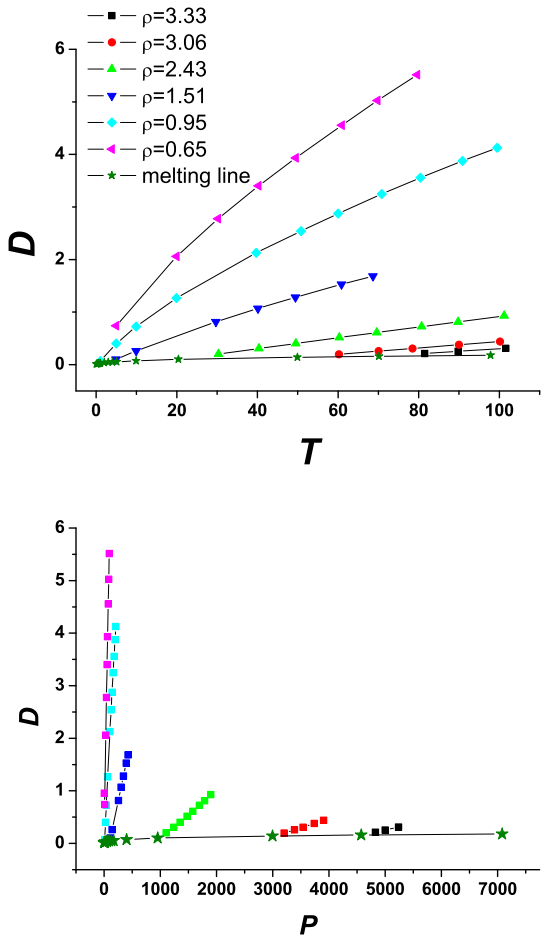

FIG. 4: Diffusion coefficient along several isochores and the melting line as functions of temperature and pressure. (Color online)

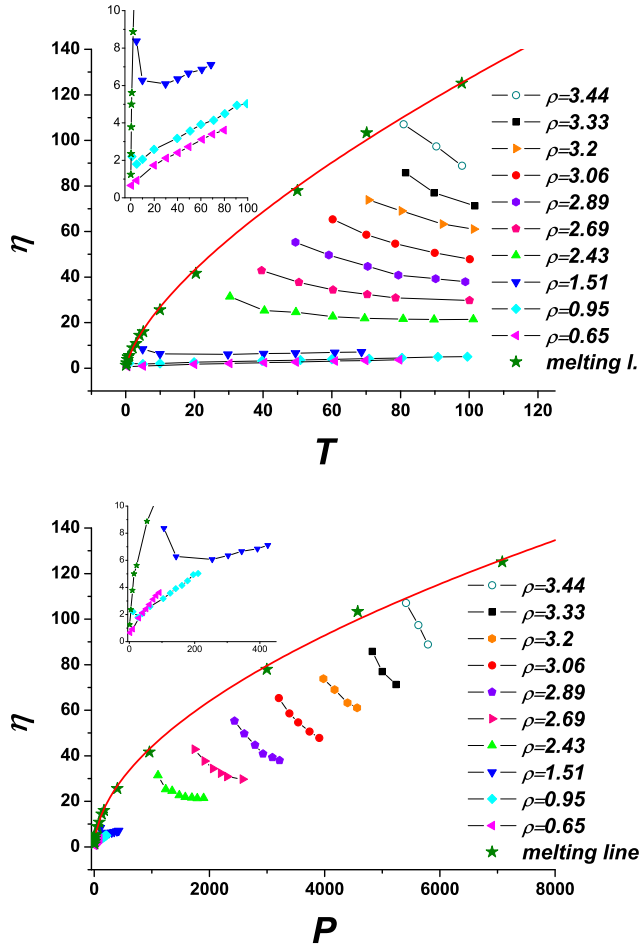

FIG. 5: Viscosity along the isochores (squares) and along the melting line (stars)as a function of pressure and temperature. The symbols are MD data and the line is the scaling law fitting. The insets represent the low pressure or low temperature behavior of the plots.(Color online)

Stokes - Einstein Relation

Given the behavior of the viscosity and diffusion coefficient, it is interesting to consider the Stokes - Einstein relation. It can be written as

$$c = \frac{k_B T}{\pi \sigma D \eta}, \tag{21}$$

where σ is the diameter of a particle and c is the constant which equal 2 for "stick" boundary conditions and 3 for the "slip" ones [17]. Several authors studied the Stokes - Einstein coefficient c in different systems [22–26]. The deviation from the Stokes - Einstein law was found. In Reference [22], a modified relation was suggested. To take into account the effect of a change of the diameter σ, it was suggested to use the relation:

$$c = \frac{k_B T}{\pi \sigma D \eta \rho^{1/3}}. \tag{22}$$

Although this normalization reduced the deviation, it did not make the coefficient c constant. The study of the Stokes - Einstein relation in the soft sphere system [24–26] also confirmed the deviation from both above formulas.

Here we apply the scaling laws to understand the Stokes - Einstein coefficient behavior. Recall that along the melting line the diffusion coefficient changes as $D \sim T^{5/12}$ while $\eta \sim T^{2/3}$. Inserting it in Eq. (22) we obtain $c \sim T^{-1/12}$. Figs. 9a and 9b represent the Stokes - Einstein coefficient c along the melting line in usual and scaled forms.

One can see that scaling law works for the Stokes - Einstein coefficient too [27]. The apparent choice for the particle size σ is the Barker diameter. For soft sphere system the Barker diameter is defined as [17, 28]:

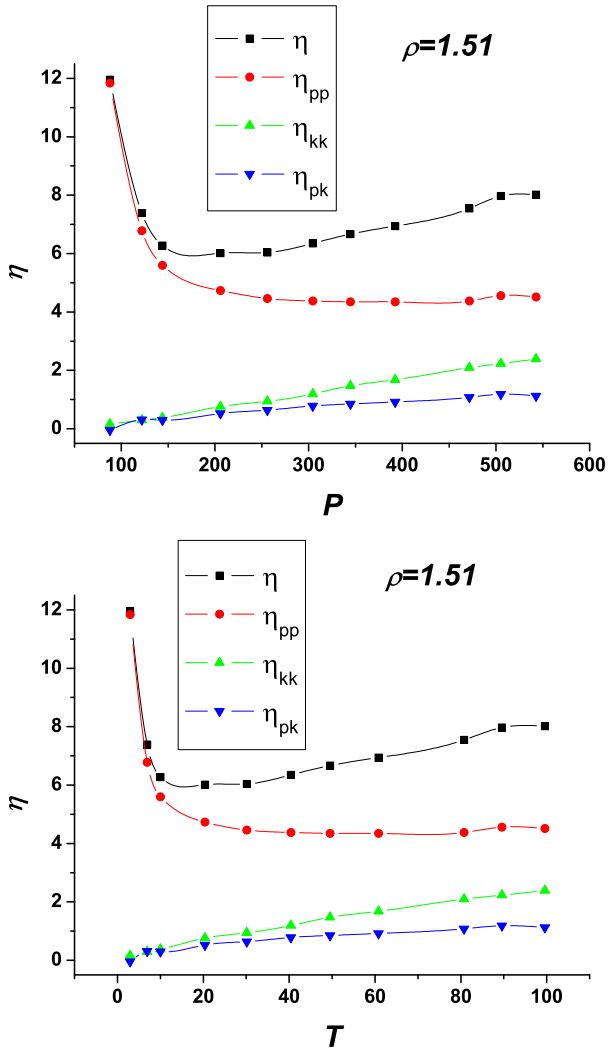

FIG. 6: Different contributions to viscosity as a function of pressure and temperature along the isochore $\rho = 1.51$. Squares - full viscosity, circles - *pp* contribution, up triangles - *kk* contribution and down triangles - *kp* contribution.(Color online)

$$d_B = \sigma \left(\frac{\varepsilon}{k_B T} \right)^{1/n} \Gamma \left(\frac{n-1}{n} \right), \qquad (23)$$

i.e. for our case $c \sim T^{-1/12}$. From this one can conclude that the Barker diameter should be used as a characteristic particle size. Fig. 10 shows $c/T^{1/12}$. One can see that the Stokes - Einstein coefficient becomes constant and equals 2 with this normalization.

Isoviscosity Lines

As it was mentioned in the introduction, the shape of the isoviscosity lines is still unclear. There are two

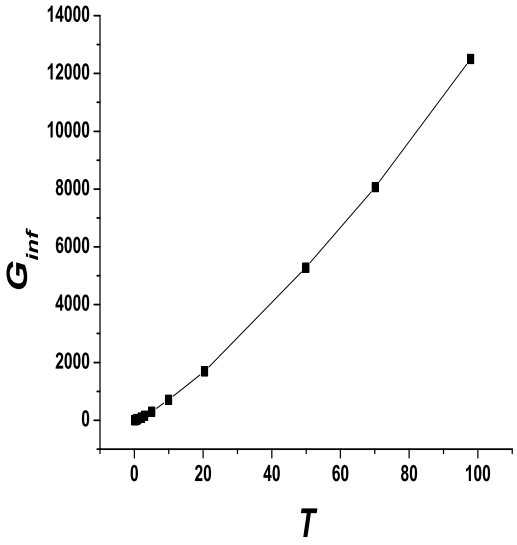

FIG. 7: Infinite-frequency shear modulus G_{inf} along the melting line.

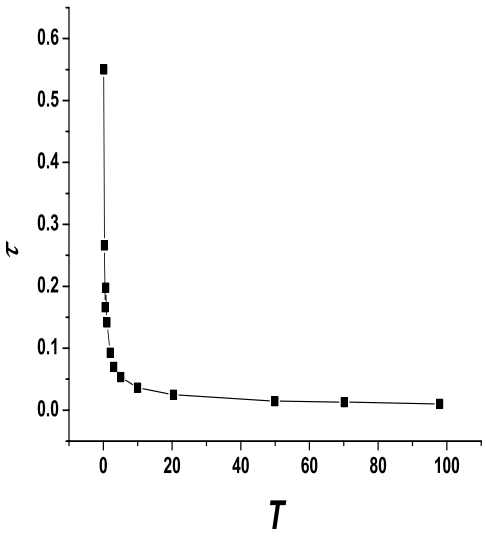

FIG. 8: Relaxation time along the melting line.

suggestions claiming that the viscosity is constant along the isochore or along the melting curve, but both of them contradict to the experimental data [4]. In this respect it is interesting to see the behavior of isoviscosity lines in the soft sphere system as a generic model for more complex liquids.

Figs. 11 and 12 present the isoviscosity lines in comparison with the viscosity along the melting line and along the isochores. One can see that the slope of the isoviscosity lines is higher then the viscosity along the

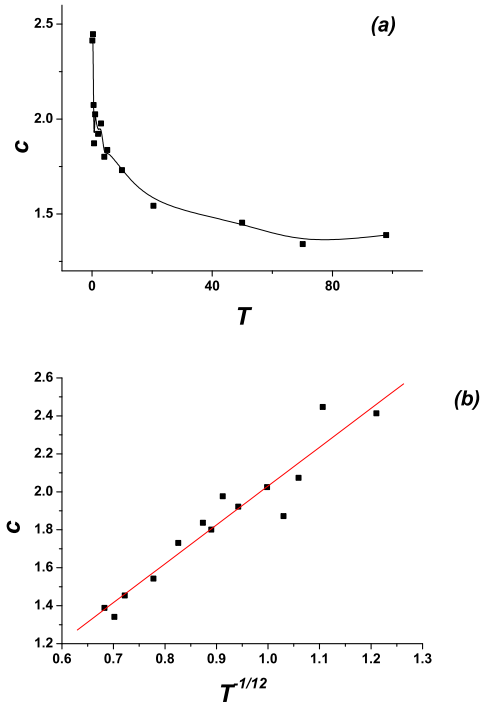

FIG. 9: Stokes - Einstein coefficient c in usual (a) and scaled (b) forms. Squares - MD results, line (b) is linear fit.

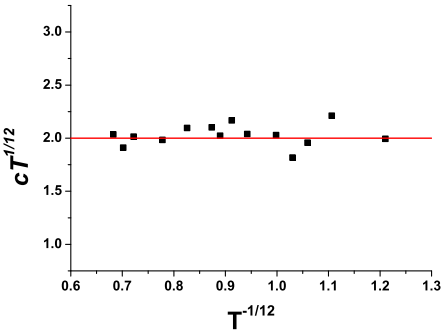

FIG. 10: Stokes - Einstein coefficient $c/T^{1/12}$.

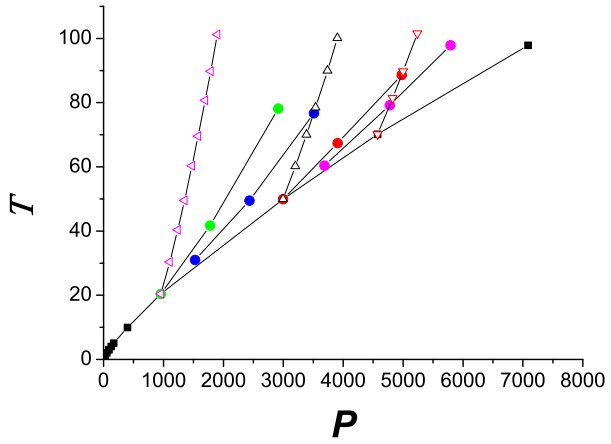

FIG. 11: Isoviscosity lines compared with the viscosity along the melting line and isochores. Squares - melting line, opened triangles - isochores (from left to right: $\rho = 2.43, 3.06$ and 3.33), filled circles - isoviscosity lines (from left to right: $\eta = 41.61, 55.32, 77.94$ and 88.86). (Color online)

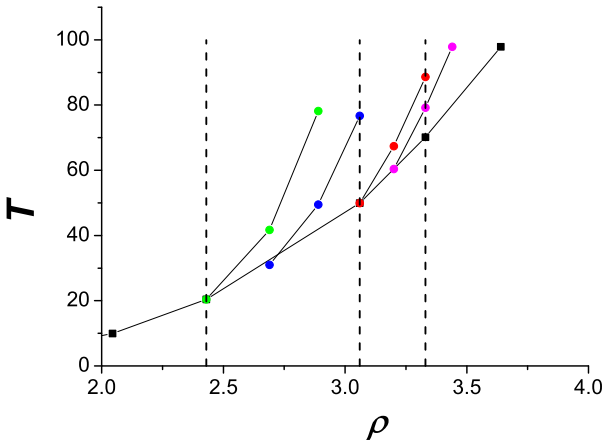

FIG. 12: Isoviscosity lines compared with the viscosity along the melting line and isochores. Squares - melting line, filled circles - isoviscosity lines (from left to right: $\eta = 41.61, 55.32, 77.94$ and 88.86). Note that the isochores are vertical lines in these coordinates (dashed lines here). (Color online)

melting line, but lower then the one along the isochores. One of us discussed the behavior of the isoviscosity lines in the previous publication [4]. Based on the experimental data for mercury and argon, it was suggested that the isoviscosity lines are located between the melting line and isochore. From this one can see that the simulation results qualitatively correspond to the experimental data.

Excess Entropy Scaling

It is important from both theoretical and practical points of view to establish some relationships between dynamic and thermodynamic properties of liquids. One of the most common relations was developed by Rosenfeld [15, 16]. According to Rosenfeld, one can define some reduced transport coefficients which exponentially depend on the excess entropy of the liquid. The reduced diffusion D^* and viscosity η^* have the following forms:

$$D^* = D\frac{\rho^{1/3}}{(k_BT/m)^{1/2}} \tag{24}$$

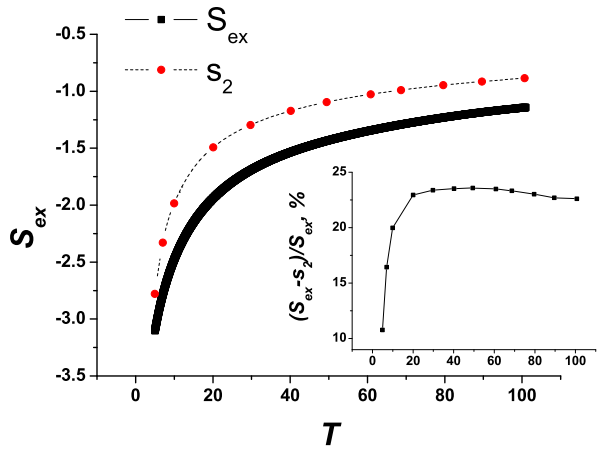

FIG. 13: Full (squares) and pair (circles) excess entropy of the soft spheres along the isochore $\rho = 1.51$. The inset represents the relative error $\frac{S_{ex}-s_2}{S_{ex}}$ in percent. (Color online)

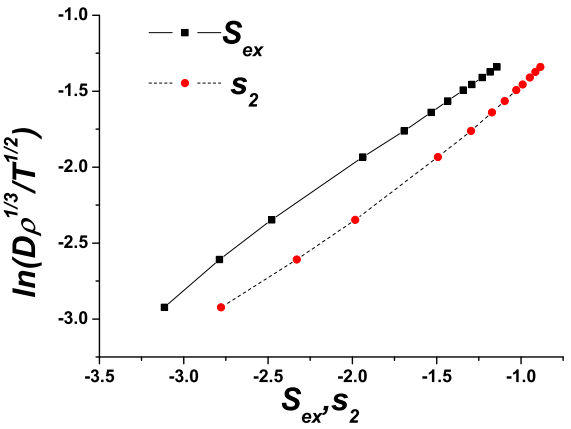

FIG. 14: Logarithm of reduced diffusion D^* as a function of full (squares) and pair (circles) excess entropy. (Color online)

$$\eta^* = \eta \frac{\rho^{-2/3}}{(mk_BT)^{1/2}}, \tag{25}$$

and their dependence on the excess entropy $S_{ex} = (S - S_{id})/(Nk_B)$ looks like

$$X = a_X \cdot e^{b_X S_{ex}}, \tag{26}$$

where X is the transport coefficient (D or η in the present case), and a_X and b_X are the constants which depend on the studied property [15, 16].

Very often one can replace the excess entropy by a pair contribution to it, which can be computed via the relation

$$s_2 = -\frac{1}{2}\rho \int d\mathbf{r}[g(\mathbf{r})\ln(g(\mathbf{r})) - (g(\mathbf{r}) - 1)], \tag{27}$$

where $g(\mathbf{r})$ is radial distribution function of the liquid.

In the present work we verify the scaling relations for the diffusion coefficient and viscosity. To do this, we calculate the pair and full excess entropies along the isochore $\rho = 1.51$. The pair excess entropy is calculated from the radial distribution function. For computing the full excess entropy, the following procedure is applied. As we mentioned above, the free energies of the system at $T = 20.0$ were calculated for determining the melting point. After that we computed the energy along the isochore $\rho = 1.51$. Having free energy at $T_0 = 20.0$ and the temperature dependence of internal energy, one can find the free energy along this isochore: $\frac{F(T)}{k_BT} - \frac{F_0}{k_BT_0} = \int_{T_0}^{T} d(\frac{1}{T'})U(T')$. The excess entropy along the isochore is obtained by differentiating the free energy with respect to temperature.

Fig.13 presents the excess entropy and pair contribution to it along the isochore $\rho = 1.51$. One can see that at some temperature the relative difference of the entropies becomes approximately constant. In the case of the exponential dependence, it gives a constant shift of the curves.

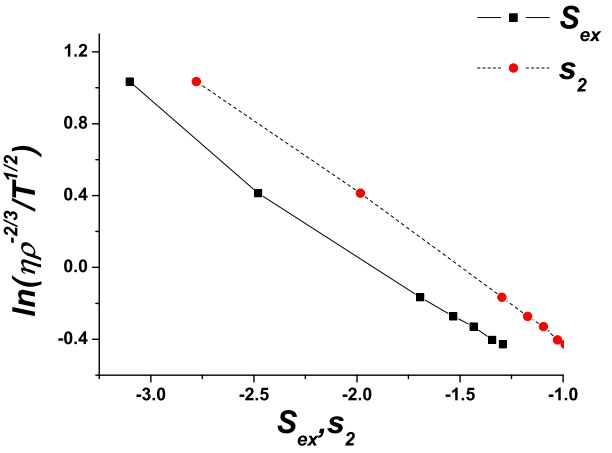

FIG. 15: Logarithm of reduced viscosity η^* as a function of full (squares) and pair (circles) excess entropy. (Color online)

Figs. 14 and 15 show the logarithm of the Rosenfeld scaled diffusion and viscosity along this isochore. As can be seen from these plots, the scaling relation is fulfilled with good accuracy in a wide range of temperatures. The curves corresponding to the full excess entropy and to the pair contribution to it have the same shape but shifted with respect to each other, which corresponds to the intuitive conclusion described above.

In conclusion to this subsection, we would like to make some remarks. First of all, recently another mechanism for the origin of the excess entropy scaling has been suggested [30]. According to this work, the scaling law is valid for the liquids with strong energy-virial correlations (the authors call them "strongly correlated liquids"). The class of strongly correlated liquids includes

many different systems, like, for example, a Lennard-Jones liquid, Kob-Andersen mixture, square-well liquid and many others. The soft spheres considered in this article are exactly the strong correlated liquids [31].

On the other hand, the applicability of the entropy scaling to not-strongly-correlated liquids is questionable. It seems that in the case of the existence of thermodynamic anomalies in the system [32, 33], Rosenfeld scaling does not work. In Ref. 34 it was shown that for Herzian spheres, Gauss Core Model, and soft repulsive shoulder potential, the Rosenfeld entropy scaling breaks down. These systems demonstrate the diffusion anomalies at low temperatures: the diffusion increases with increasing density or pressure. It is shown that for the first two systems, which belong to the class of bounded potentials, the Rosenfeld scaling formula is valid only in the infinite temperature limit where there are no anomalies. For the soft repulsive shoulder, the scaling formula is valid already at sufficiently low temperatures, however, out of the anomaly range.

Influence of Attraction

Finally we would like to study the influence of attractive forces on the behavior of the viscosity. To do this, we simulate the Lennard-Jones like system. The system has the potential function:

$$\Phi_{LJ} = \varepsilon \cdot [(\frac{\sigma}{r})^{12} - (\frac{\sigma}{r})^{6}] \qquad (28)$$

with the parameters $\varepsilon = 1$ and $\sigma = 1$.

We measure the viscosity of both LJ systems at the isochore $\rho = 1.51$. The resulting curves are shown in Figs. 16a and 16b. One can see from these figures that the difference takes place only in the low temperature region and should be concerned to the *pp* contribution while at high temperatures where *kk* contribution is dominant the viscosity of soft spheres and LJ system have very close magnitudes.

Based on these results, one can expect that in the case of real liquids the viscosity can demonstrate complex behavior on compression, since they are characterized by complex non pair potentials which can even be state dependent. The results for the soft sphere system can directly be applied only for the rare gas liquids, although even in this case the attraction is important, as is seen from Figs. 16a and b.

As one can see from the figures the difference between the soft spheres and Lennard-Jones system takes place only in the low temperature regime. One can attribute it to the difference in potential - potential contribution to the viscosity while at high temperature the influence of the kinetic - kinetic term is not so strongly affected by the interatomic potential.

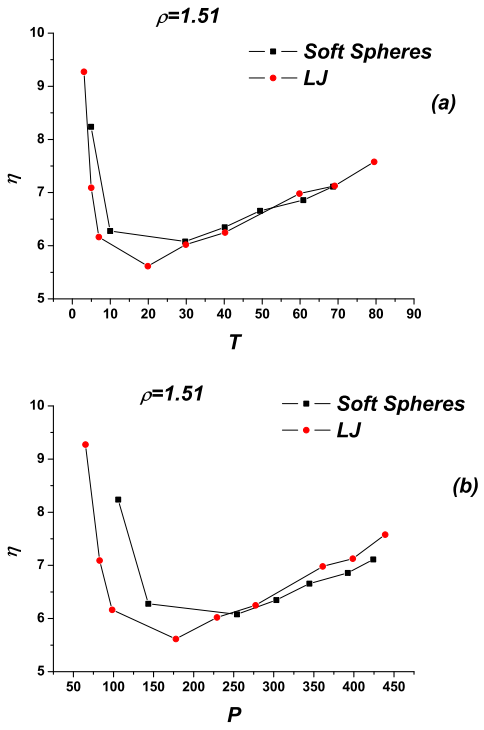

FIG. 16: Viscosity of the soft sphere and Lenard-Jones systems along the isochore $\rho = 1.51$. Squares - soft spheres, and circles - LJ. (Color online)

IV. CONCLUSIONS

In conclusion we have carried out a comprehensive study of the viscosity and diffusivity of the soft sphere system. We showed the validity of the scaling laws along the melting line. We proposed the scaling law for the Stokes - Einstein coefficient and verified it. The influence of different contributions to the viscosity was discussed. It was shown that the viscosity is strongly growing along the melting line, however, this growth does not stimulate the glass transition because the relaxation time is decreasing. We calculated the shape of the isoviscosity lines and compared them with the viscosity along the melting line and isochores. The results we obtained are qualitatively similar to the experimental findings. The validity of the Rosenfeld excess entropy scaling was also verified. Interestingly, although the qualitative behavior of viscosity and diffusivity is rather different, the excess entropy scaling describes both coefficients with high accuracy. Finally, the influence of the attractive forces was verified via the comparison to the Lenard-Jones system. It was shown that the attraction is important only at sufficiently low temperatures.

We thank S. M. Stishov, E. E. Tareyeva and A. G. Lyapin for stimulating discussions. Y.F. thanks the Joint Supercomputing Center of the Russian Academy of Sci-

ences for computational power. The work was supported in part by the Russian Foundation for Basic Research (Grant No 08-02-00781).

[1] V. V. Brazhkin, J. Phys.: Condens. Matter **20**, 244102 (2008).
[2] P. W. Bridgman, Collected Experimental Papers vol VI (Cambridge, MA: Harvard University Press) p. 2043 (1964).
[3] J. P. Poirier, Geophys. J. **92**, 99 (1988).
[4] V.V. Brazhkin and A.G. Lyapin, Physics-Uspekhi, **170**, 535 (2000).
[5] D. P. Dobson, Phys. Earth Planet. Interiors **130**, 271 (2002).
[6] H. Terasaki et al, Geophys. Res. Lett. **33**, L22307 (2006).
[7] S. Bastea, Phys. Rev. E, **68**, 031204 (2003)
[8] D. Frenkel, B. Smit. "Understanding Molecular Simulation", Academic Press (2002).
[9] T.H. Berlin and E.W. Montroll, J. Chem. Phys. **20**, 75 (1952).
[10] O. Klein, Medd. Vetenskapsakad. Nobelinst. **5**, No. 6 (1919).
[11] S.M. Stishov, Physics-Uspekhi, **114**, 1 (1974).
[12] V. V. Zhakhovsky, Zh. Eksp. Teor. Fiz. **105**, 1615 (1994)[JETP **105**, 1615 (1994)].
[13] W.G. Hoover, M. Ross and K. W. Jonson, Journal of Chemical Physics. **52**, 4931 (1970).
[14] B. B. Laird and D. M. Kroll, Phys. Rev. A **42**, 4810 (1990).
[15] Ya. Rosenfeld, J. Phys. Condens. Matter **11**, 5415 (1999).
[16] Ya. Rosenfeld, Phys. Rev. A **15**, 2545 (1977).
[17] J.-P. Hansen, I.R. McDonald. "Theory of simple liquids", Academic Press (1986).
[18] H. Stassen and W. A. Steele, J. Chem. Phys. **102**, 932 (1994)
[19] K. Meier, A. Laesecke and St. Kabelac, J. Chem. Phys. **121**, 3671 (2004).
[20] D.M. Heyes, Phys. Chem. Liq., **20**, 115 (1989)
[21] R. Zwanzig and R.D. Mountain, J. Chem. Phys. **43**, 4464 (1965)
[22] R. Zwanzig, J. Chem. Phys. **79**, 4507 (1983)
[23] N.H. March and J.A. Alonso, Phys. Rev. E **73**, 032201 (2006).
[24] D.M. Heyes, J. Phys.: Condens. Matter, **19**, 376106 (2007).
[25] D.M. Heyes and A.C. Branka, Phys. Chem. Chem. Phys. **9**, 5570 (2007).
[26] D.M. Heyes and A.C. Branka, J. Phys.: Condens. Matter **20**, 115102 (2008).
[27] The noise in the Stokes - Einstein coefficient is because of the errors in the viscosity computation.
[28] J. A. Barker and D. Henderson, Rev. Mod. Phys. **48**, 587 (1976).
[29] M. Dzugutov, Nature **381**, 137 (1996).
[30] N. Gnan, T. B. Schrøder, U.R. Pedersen, N.P. Bailey and J.C. Dyre, J. Chem. Phys. **131**, 234504 (2009).
[31] T.B. Schroder, N.P. Bailey, U.R. Pedersen, N. Gnan, and J.C. Dyre, J. Chem. Phys. **131**, 234503 (2009).
[32] Yu. D. Fomin, N. V. Gribova, V. N. Ryzhov, S. M. Stishov, and Daan Frenkel, J. Chem. Phys. **129**, 064512 (2008).
[33] N. V. Gribova, Yu. D. Fomin, Daan Frenkel, V. N. Ryzhov, Phys. Rev. E **79**, 051202 (2009).
[34] Yu.D. Fomin, N. V. Gribova, and V. N. Ryzhov, arXiv:1001.0111v1.